Journal of Non-Crystalline Solids 147&148 (1992) 206–212
North-Holland

JOURNAL OF
NON-CRYSTALLINE SOLIDS

Ultrastructural evolution during gelation of TiO_2–SiO_2 sols

M. Ramírez-del-Solar [a], L. Esquivias [a], A.F. Craievich [b] and J. Zarzycki [c]

[a] *Department of Structure and Properties of the Materials, University of Cádiz, Apdo. 40, Puerto Real 11510, Cádiz, Spain*
[b] *Laboratorio Nacional de Luz Sincrotron / CNPq, Campinas, SP, Brazil and Instituto de Física / USP, Sao Paulo, Brazil*
[c] *Laboratory of Science of Vitreous Materials (LA1119), University of Montpellier II, 34060 Montpellier cedex, France*

Small angle X-ray scattering was used to examine in situ formation of mixed TiO_2–SiO_2 gels. In order to elaborate the homogeneous solution, either ultrasonic radiation or alcoholic dilution of the precursors was carried out. The evolution of the typical sizes calculated at low and high q-regions were correlated. This lead to an approximate model for the aggregation process. The fit of the experimental data to a simple growth law was attempted allowing a kinetic rate constant to be estimated. This permits the evaluation of the differences induced in titanium doped silica sono- and classic gels.

1. Introduction

The sol–gel process is frequently applied to synthesize ceramics and glasses of a great variety of systems. In order to facilitate the control of final material properties, an integrated study of the different aggregation states from the initial colloidal solution is essential. In previous papers [1–3], the physico-chemical and structural characteristics of sonogels were compared with those of standard gels obtained with alcoholic dilution. These studies were undertaken after the gel point, but a complete investigation of this mechanism requires investigation of the 'sonosol to sonogel' transition.

Analysis of a gelling solution needs an 'in situ' method such as NMR, vibrational spectroscopy or small angle scattering. Small angle X-ray scattering (SAXS) was used to probe the structure and growth kinetics of the macromolecular networks of pure and titania-doped silica sono- and classic sols before gelation. This technique measures the angular dependence of the intensity scattered by a sample with heterogeneities in electron density. At low angles, the scattered intensity from isolated aggregates can be approximated by Guinier's law [4]:

$$I(q) = I(0)\,\exp\left(-\frac{Rg^2q^2}{3}\right), \tag{1}$$

where $I(0)$ is the extrapolated intensity to $q = 0$, R_g is the radius of gyration of the aggregates and $q = (4\pi/\lambda)\sin(\theta/2)$ is the modulus of the scattering vector; λ and θ are the X-ray wavelength and scattering angle, respectively. Analysis of this region of the scattering curves and their time evolution provides information about the overall size and mechanism of cluster growth [5]. The asymptotic behaviour, for large q, is described by Porod's law ($I \sim q^{-4}$) provided the system has sharp interfaces [4]. If aggregates are mass fractals, the intermediate q-range exhibits a potential dependence [6]:

$$I(q) \propto q^{-x}, \tag{2}$$

where x is the fractal dimension D, which can be determined from the linear part of a log I versus log q plot. A crossover between these two domains and the asymptotic (Porod) q-region are usually observed. This crossover, located at $q = q_m$, defines a parameter, R', corresponding to the size of the primary particles which comprise the fractal aggregate ($R' = 1/q_m$).

2. Experimental

2.1. Sample preparation

Gels of the composition $x\mathrm{TiO_2}$–$(100-x)\mathrm{SiO_2}$ were made by mixing solutions of oxides precursors tetraethoxysilane (TEOS) and tetrabutylorthotanate (TBOT). The chemical reactions were carried out under acidic conditions with pH[HCl] = 1.5. The classic hydrolysis of TEOS is accomplished by stoichiometric additions of water (4 mol/mol alkoxide) in an alcoholic (EtOH) environment, under magnetical stirring, while in the sonocatalytic method the solventless TEOS–water mixture is subjected to ultrasonic radiation [3].

In both cases, once the solutions were cooled to 0°C, appropriate volumes of a titanium precursor solution TBOT : AcOH : nBuOH (1 : 5.5 : 3.5), in which AcH behaves as titanium alkoxide chemical modifier, were added under vigorous stirring to obtain different compositions. Sono- and classic mixed solutions are labelled as xSm and xCm, respectively, x being 0, 1 or 5 (the nominal TiO_2 molar content) and m corresponds to the relative t/t_g time where t_g is the gelation time.

2.2. Small angle X-ray scattering

Small angle X-ray scattering measurements were performed at the small angle scattering station of the synchrotron radiation laboratory LURE, Orsay, France, using a pin-hole collimated X-ray beam. A suitable wavelength was selected (λ = 1.4 Å) using a Ge(111) bent monochromator. For the SAXS experiments, the solutions were poured into a bronze cell between two Mylar windows. The sample thickness, t, was chosen to be $t = 1/\mu$, μ being the linear absorption coefficient, in order to obtain the maximum in the scattered intensity [4]. The cell was placed in a thermostated block maintained at 60°C during the aggregation and gelation processes. Recording of scattered intensities at fixed intervals provides useful information that can be correlated with the evolution of microstructure. The gelation time, t_g, of the solutions was previously measured in similar cells, for each composition in the same conditions (table 1).

The scattered X-ray intensities were recorded as a function of scattering angle using a one-dimension position-sensitive detector. Parasitic scattering was measured using a blank sample with an empty cell. For samples with a faster gelation kinetics (5S, 5C and 1S), the spectra were obtained continuously with acquisition times ranging from 3 to 5 min. For the slower ones, data were taken at various intervals, depending on the sample, with counting times of 5 min.

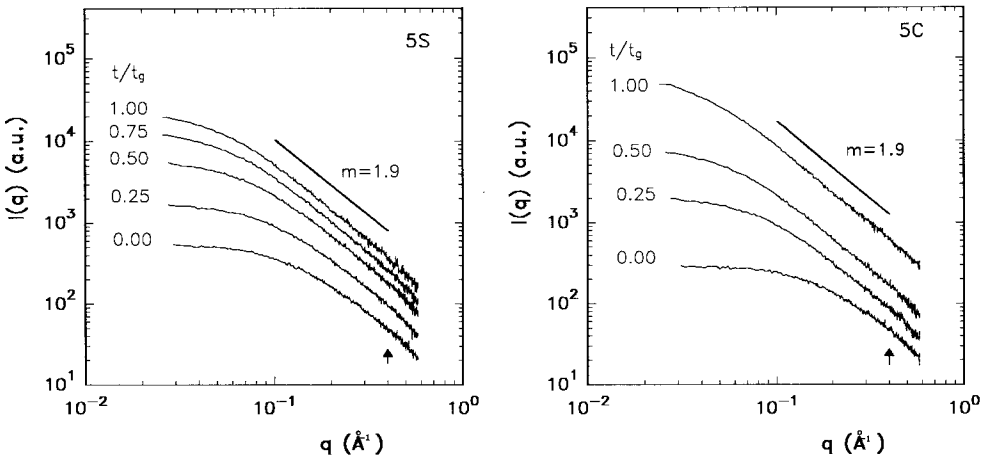

Fig. 1. Development of the scattering profiles for sono- and classic $5\mathrm{TiO_2}$–$95\mathrm{SiO_2}$ solutions at different stages of polymerization. Notice the change of the final slope of the curves at the high q-region indicated. (Curves have been vertically displaced the same relative distance for a more clear visualization.)

3. Structural features

Figures 1(a) and (b) show representative sets of curves obtained at different aggregation times for 5% TiO_2 sols. The overall behaviour of SAXS curves indicates an increase of the q-range showing a power–law decay with aggregation. Close to the gel point ($t/t_g \approx 1$), most of the curve domain is consistent with a q power–law. The calculated slopes related to internal structure of aggregates indicate that the local geometric structure is unchanged during the sol–gel transition [4]. The linearity of the log I versus log q plots for a wide q-domain is consistent with the behaviour ex-

Table 1
Several characteristic parameters measured for both series of sono- and classic solutions

X	t_g (min)	D	D'	$R_g(t_g)$ (Å)
0S	390	1.82	–	17
1S	105	1.92	1.73	22
5S	30	1.99	1.88	45
0C	1800	1.73	–	58
1C	300	1.90	–	109
5C	140	1.93	1.75	41

Gelation time at 60°C, dimensionalities calculated from final slope of fresh gel scattering curves, those averaged during the aggregation process from $I(0) = f(R_g)$ dependence and gyration radius of fresh gels.

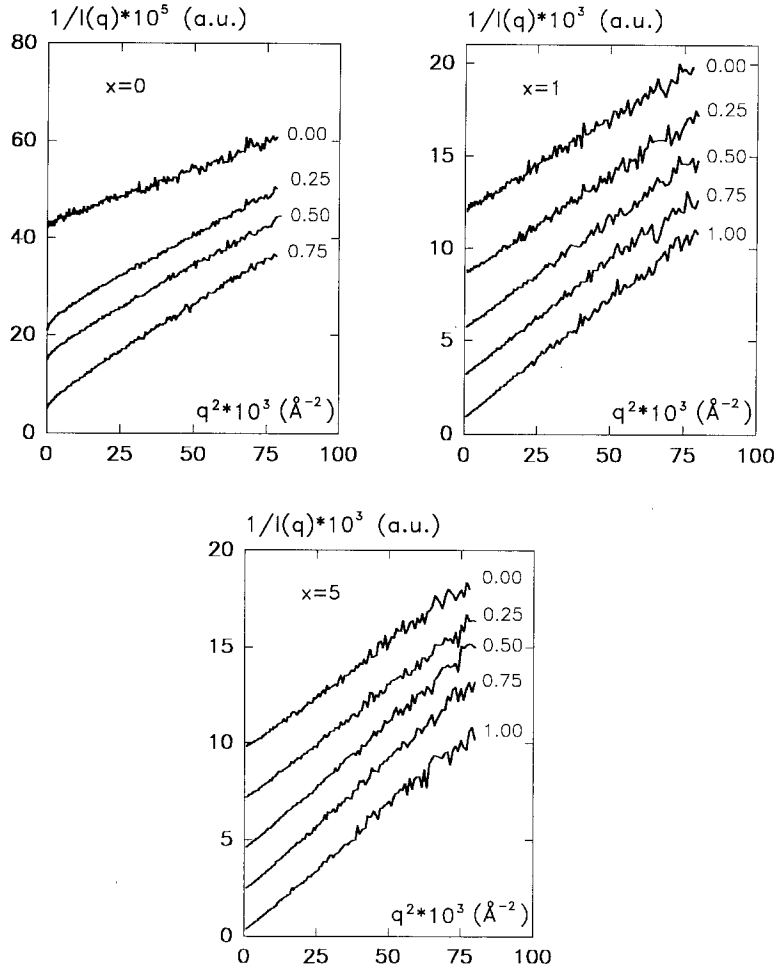

Fig. 2. Zimm plots for three sonosolutions containing x% TiO_2 and for the t/t_g values indicated on each right side. (Curves have been vertically displaced the same relative distance for a more clear visualization.)

pected for mass fractal structures. This linearity extends to a maximum q_m value at which a crossover is theoretically expected. This behaviour is associated with the size, R', of the primary particles by $R' = 1/q_m$. The experimental curves yield $R' \approx 2.5$ Å.

As aggregation proceeds, clusters become much larger than monomers, causing a widening of the linear domain of the log–log curves. Thus, more precise linear regressions are found from the scattering intensity plots corresponding to fresh gels of all compositions. The effect of titanium on the SiO_2 structure produces an increase in the exponent x of eq. (2) (table 1) and, consequently, in the fractal dimensionality, D. This suggests a more compact network occurs with increasing TiO_2 content. However, comparisons between these D-values must be made with care because of small differences in the aging time of each gel.

Since a saturation of the scattered intensity at low q is observed, an analysis of this region on the basis of the Guinier approximation (eq. (1)) was attempted. However, owing to the limited approximation validity ($qR_g \ll 1$), linear regressions in the log $I(q) - q^2$ plots are only possible at early stages in the reaction and within a narrow q-range. The variation in the scattered experimental intensities at low q was fitted using the Zimm approximation which holds for polymeric-ball like particles. Better agreement was observed with the Zimm equation [7]:

$$\frac{1}{I(q)} = \frac{1}{I(0)}\left[\left(1 + \frac{q^2 R_g^2}{3}\right)\right] \tag{3}$$

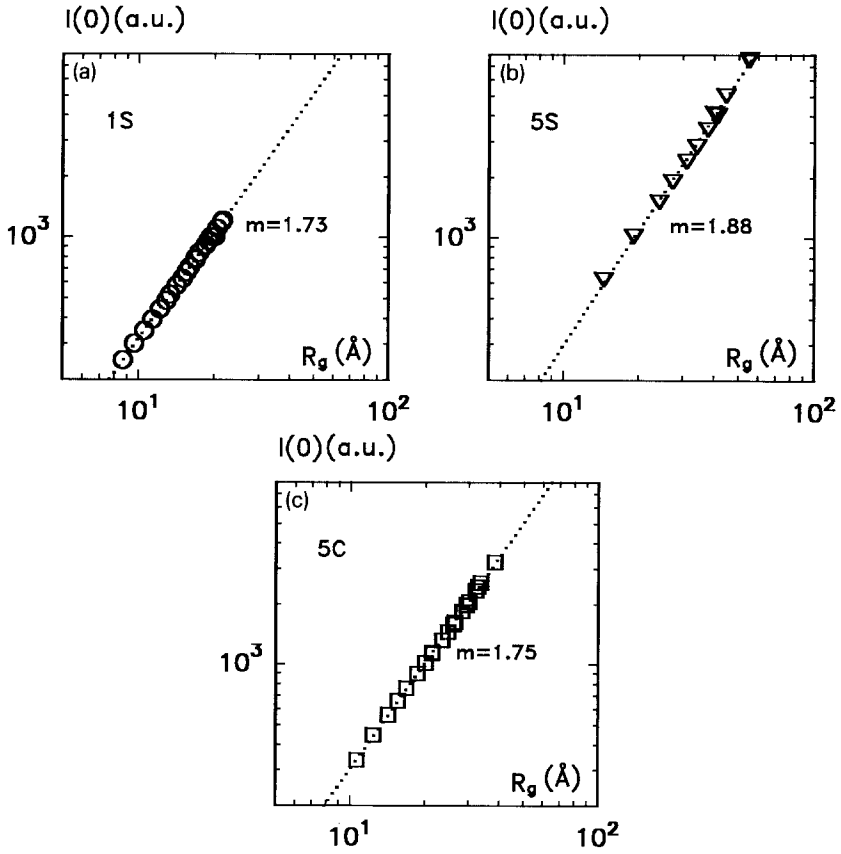

Fig. 3. Variation of the extrapolated intensity, $I(0)$, with the average radius of gyration, R_g.

and $I(0)$ and R_g can be evaluated from the wide linear regions in fig. 2 for the three sonosolutions.

Logarithmic plots of $I(0)$ versus R_g values provide additional information about solution structure. This analysis has been made for samples with a gelation times that permit continuous study in situ. Figure 3 data show the evolution of $I(0)$, which is proportional to the aggregate mass, as a function of their average size parameter, R_g. These log–log plots should display linear behaviour when the extrapolated SAXS intensity, $I(0)$, is related to R_g by [4]

$$I(0) \propto R_g^D. \quad (4)$$

This equation applied to growing mass fractal objects. The slopes of fig. 3 plots indicate the presence of slightly branched polymeric clusters [8], in agreement with the previous results. The dimensionality, D, calculated from the slopes of log I versus log q plots for fresh gels are a little higher than D' determined from log $I(0)$ versus log R_g plots. The last ones (D') are average values during cluster growth. So, differences between D and D' indicate that fractal dimensionality increases during aggregation, suggesting that a restructuring process is also acting. Dimensionalities are expected to be higher in processes involving restructuring than in those involving only pure aggregation [9].

In order to obtain further details of the aggregation process, the evolution of the integral invariant, Q_0, was determined. This integral parameter, when applied to a 'two-density' material, is related to its structure by [4]

$$Q_0 = \int_0^\infty I(q)q^2 \, dq = 2\pi^2(\Delta\rho)^2\phi(1-\phi)V, \quad (5)$$

where $\Delta\rho$ is the difference in electronic density between the phases, ϕ is the volume fraction of one of the phases and V is the irradiated volume.

For evaluation of eq. (5), appropriate extrapolations for $q \to 0$ and $q \to \infty$ must be done [10]. For $q \to 0$, the extrapolation is easily accomplished using Zimm plots. For $\theta \to \infty$, it is assumed that, after the crossover found, the SAXS intensity for $q > q_{max}$ (q_{max} being the maximum q-value for which the intensity was recorded) exhibits a Porod behaviour [4], i.e., $I(q)q^4 = k_p$,

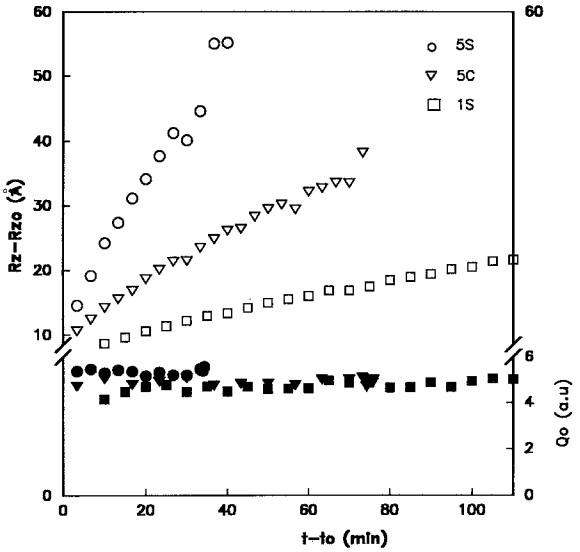

Fig. 4. Evolution during gelation time of the gyration radius calculated from Zimm plots (open symbols) and the integral invariant (filled symbols).

k_p being a constant. The contribution of the Porod's region is small for all the experimental curves except those corresponding to very short reaction time.

The integral invariant, Q_0, was calculated from the curves measured in a larger q-domain (5c, 5s and 1s), for which a reasonable extrapolation, beyond the experimental q-range is possible. The integral values, which are plotted in fig. 4, do not vary noticeably during aggregation and, hence, the total volume fraction of the scatterers is also constant. Gelation of these solutions is concluded to occur by a cluster–cluster aggregation process.

The surface/volume ratio of the scatterers can be determined as the ratio K_p/Q_0, but a particular geometry should be assumed in order to estimate their characteristic dimension. In this sense, attention must be paid to the fact that there is no evolution with time of the V/S ratio. Consequently, we can rule out the formation of spherical particles (or voids), the growth of which would imply an increase of this parameter as R_g does. It seems more appropriate to describe the internal structure on the basis of rod-like scatterers which lengthen with an essentially constant cross-section.

4. Kinetic of aggregation

The evolution of the correlation length, R_g, calculated at the lower angles, i.e., larger distances, is apparent in fig. 4. It is clear that the wide angular domain explored makes accessible two characteristic dimensions (R_g and R') of the system which allow a more detailed investigation. A tentative model of the growing clusters, which is consistent with the above structural considerations and this behaviour, is represented in fig. 5. In such polymeric-like clusters, the cross-dimension, R', of the elementary particles (or voids) remains unchanged, at least on gelation, while there is aggregation due to their lengthening which generate clusters with rising size, R_g. The increase in the fractal dimension indicates that internal restructuring and, probably, coalescence of the filaments occurs, leading to densification during aging.

The time evolution of the clusters size can usually be described on the basis of a growth law [11]:

$$R_g - (R_g)_0 = K(t - t_0)^{\alpha}. \quad (6)$$

Log–log plots of the gyration radius versus time permit estimation of the kinetic rate constant of the process, K, and the constant α. Figure 6 presents results on systems analyzed which fit this law. The K-values confirm that both the increase of the TiO_2 content and the supply of ultrasound increases aggregation rate. The constant α is the same for all samples. This would indicate that the aggregation mechanism does not change with composition. In a simple aggregation model we expect $\alpha = 1/D$. The value of D obtained from fig. 6 plots ($D \approx 1.2$) is much slower than that obtained using the log–log and $I(0)$ versus R_g plots. Therefore we conclude that the approximation $\alpha = 1/D$ does not apply to the system studied.

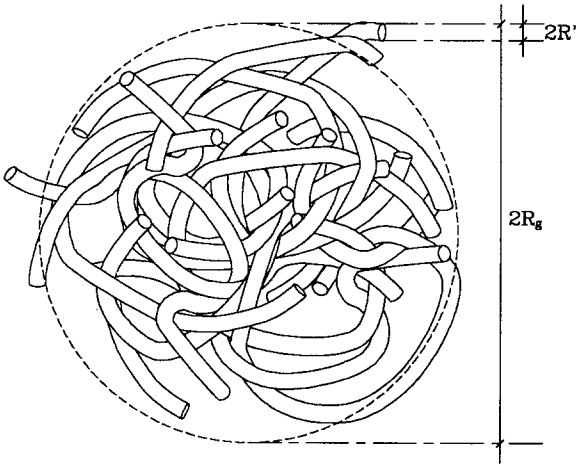

Fig. 5. Schematic illustration of the model proposed for mixed titania–silica gelling systems.

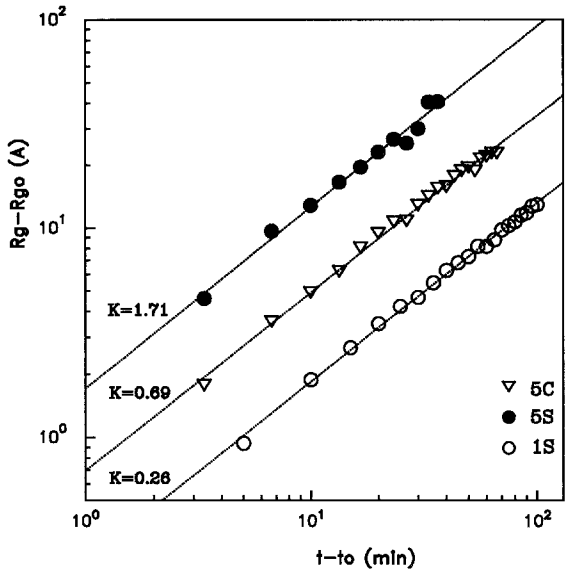

Fig. 6. Fitting of the time dependence of the gyration radius before the gel point to a law of growth like $\log[R_g - R_g(0)] = \log K + 1/D \log t$. Notice the augmentation of the extrapolated value ($\log K$) when increasing x and ultrasounds are applied.

5. Conclusion

This SAXS study of titania-doped sono- and classic silica sols reveals that the local geometric structure of aggregates remains unchanged during gelation. Analysis provides the kinetics of two characteristic scatterer length from which a structural model can be inferred. This model is consistent with the mass fractal growth behaviour de-

duced from the time evolution of the scattering profiles.

The evolution was described on the basis of a simple growth law that allows estimation of the process rate constant. The values obtained confirm that both the increase of TiO_2 content and ultrasound accelerate aggregation.

The authors gratefully acknowledge the assistance of Dr de la Rosa-Fox in computational calculations and Mr J. González in graphic designs. This work has been supported by Plan Nacional F.P.I. (Spain) and CNPq (Brazil).

References

[1] L. Esquivias and J. Zarzycki, in: Ultrastructure Processing of Advanced Ceramics, ed. J.D. Mackenzie and D.R. Ulrich (Wiley, New York, 1987) p. 255.
[2] J. Zarzycki, in: 4th Int. Conf. on Ultrastructure Processing of Ceramics, Glasses and Composites, Tucson AZ, 1989.
[3] M. Ramírez del Solar, N. de la Rosa-Fox, L. Esquivias and J. Zarzycki, J. Non-Cryst. Solids 121 (1990) 84.
[4] O. Glatter and O. Kratky, Small Angle X-Ray Scattering (Academic Press, New York, 1982).
[5] D.W. Schaefer and K.D. Keefer, Phys. Rev. Lett. 53 (1984) 1383.
[6] D.W. Schaefer, Mater. Res. Soc. Bull. 8 (1988) 22.
[7] B.H. Zimm, J. Chem. Phys. 16 (1948) 1093.
[8] C.J. Brinker, K.D. Keefer, D.W. Schaefer, R.A. Assink, B.D. Kay and C.S. Ashley, J. Non-Cryst. Solids 63 (1984) 45.
[9] R. Jullien and R. Botet, Aggregation and Fractal Aggregates (World Scientific, Singapore, 1987).
[10] M. Ramírez-del-Solar, PhD thesis, University of Cádiz (1991).
[11] T. Lours, J. Zarzycki, A. Craievich, D.I. Dos Santos and M. Aegerter, J. Non-Cryst. Solids 100 (1988) 207.